

Fabrication and Characterization of PEO/PPC Polymer Electrolyte for Lithium-Ion Battery

Xiao-Yuan Yu, Min Xiao, Shuang-Jin Wang, Qi-Qiang Zhao, Yue-Zhong Meng

State Key Laboratory of Optoelectronic Materials and Technologies, Institute of Optoelectronic and Functional Composite Materials, Sun Yat-Sen University, Guangzhou 510275, People's Republic of China

Received 14 June 2008; accepted 18 December 2008

DOI 10.1002/app.29915

Published online 26 October 2009 in Wiley InterScience (www.interscience.wiley.com).

ABSTRACT: A new poly(propylene carbonate)/poly(ethylene oxide) (PEO/PPC) polymer electrolytes (PEs) have been developed by solution-casting technique using biodegradable PPC and PEO. The morphology, structure, and thermal properties of the PEO/PPC polymer electrolytes were investigated by scanning electron microscopy, X-ray diffraction, and differential scanning calorimetry methods. The ionic conductivity and the electrochemical stability window of the PEO/PPC polymer electrolytes were also measured. The results showed that the T_g and the crystal-

linity of PEO decrease, and consequently, the ionic conductivity increases because of the addition of amorphous PPC. The PEO/50%PPC/10%LiClO₄ polymer electrolyte possesses good properties such as $6.83 \times 10^{-5} \text{ S cm}^{-1}$ of ionic conductivity at room temperature and 4.5 V of the electrochemical stability window. © 2009 Wiley Periodicals, Inc. *J Appl Polym Sci* 115: 2718–2722, 2010

Key words: polymer electrolyte; lithium-ion battery; electrochemical property; PEO

INTRODUCTION

Polymer electrolytes have received considerable attention because of the vast potential application in advanced electrochemical devices such as lithium-ion batteries and superior capacitor.^{1–4} In various batteries, polymer electrolyte not only serves as electrolytes but also as separator between anode and cathode. Therefore, superior properties of polymer electrolytes such as high ionic conductivity, wide electrochemical window, good dimensional stability, sufficient thermal stability, good mechanical stability, and high electrochemical stability are expected by researches.

Recently, several polymer electrolytes (PEs) with high ionic conductivity based on poly(ethylene oxide) (PEO), poly(vinylidene fluoridehexafluoropropylene) (PVDF-HFP), and poly(methyl methacrylate)(PMMA) have been reported.^{5–10} However, the properties of

currently used polymer electrolytes are still not satisfied enough to meet the applicable requirement. The remaining problems include the ionic conductivity at low ambient and subambient temperature, low lithium cation transference number, and formation of highly resistive layers at polymer electrolyte–lithium electrode interface. Intensive efforts have been devoted to modify the structure and properties of polymeric electrolyte concerning the aforementioned limitations.^{11–13} As a crystalline polymer, PEO shows good mechanical properties but low ionic conductivity ($10^{-8} \text{ S cm}^{-1}$) at room temperature. To enhance the ionic conductivity, the PEO-based polymer electrolytes have been extensively studied.^{14,15} Amorphous PEO salt complexes show high ionic conductivity when compared with crystalline PEO salt complexes, probably because of the easier segmental motion of the polymeric chain during ion transportation. Some works have been reported to decrease the crystallinity of polymer.^{16,17} The copolymers of PEO and the PEO composites containing other polymers or inorganic supports were used as solid polymer electrolytes (SPEs), and these SPEs showed decreased crystallinity of PEO.^{18–21}

In this work, a new PEO-based SPE-containing biodegradable amorphous poly(propylene carbonate)(PPC) was first reported. PPC has attracted increasing attention because of its biodegradability in natural surrounding.²² In this sense, the biodegradable polymer electrolyte can decrease the environmental pollution from battery disposal.

Correspondence to: Y.-Z. Meng (mengyzh@mail.sysu.edu.cn).

Contract grant sponsor: China High-Tech Development 863 program; contract grant number: 2007AA032217.

Contract grant sponsor: Guangdong Science and Technology Bureau; contract grant numbers: 2003C105004, 2006B12401006.

Contract grant sponsor: Guangzhou Science and Technology Bureau; contract grant number: 2005U13D2031.

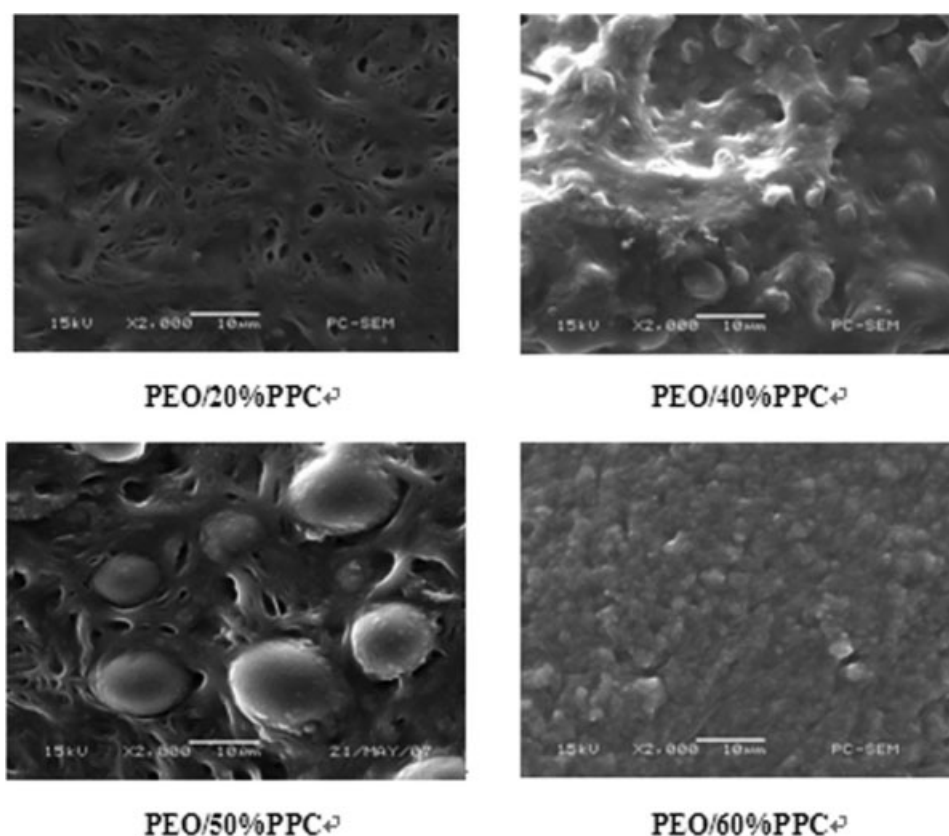


Figure 1 SEM micrographs of the cross section of PEO/*x*%PPC polymer electrolytes.

EXPERIMENT

Materials

The PPC ($M_w = 50,000$) used in this work was prepared in our laboratory. The PEO ($M_w = 620,000$) was purchased from Shanghai Liansheng Chemical (Shanghai, China). Battery-grade LiClO_4 was dried under vacuum oven at 120°C for 24 h before use.

Preparation of PEO/PPC polymer electrolyte

The PEO/PPC polymer electrolytes were prepared by solution-casting method, which involved the first dispersion of LiClO_4 in anhydrous acetone at room temperature, followed by the addition of PPC and PEO. After stirring for 24 h at room temperature, the resulting homogeneous solutions were cast onto a PTFE plate. Most of the solvents was evaporated at room temperature, and then the polymer films were dried at 60°C in a vacuum oven for 24 h to remove the remaining solvent. Finally, the PEO/PPC polymer electrolyte with thickness ranging from 100 to $150\ \mu\text{m}$ was obtained. The PEO/PPC polymer electrolyte was denoted as PEO/*x*%PPC, in which Li to the total of PEO and PPC ratio was fixed to 10 wt % for all samples, and the content of PPC, *x*, ranged from 20 to 70 wt % of PEO and PPC.

Measurements

SEM images of the cross section of PEO/PPC polymer electrolyte were observed in JEOL JSM-6380LA with gold sputter-coated films. Electrolytes films were broken in liquid nitrogen to obtain a cross section.

Differential scanning calorimetry (DSC) examination of the PEO/PPC polymer electrolytes was carried out on a NETZSCH DSC-200PC instrument at a heating rate of $20^\circ\text{C}\ \text{min}^{-1}$ from -50 to 100°C in the heating cycle and from 100 to -50°C in the cooling cycle under nitrogen atmosphere. The second scan was immediately initiated after the sample was cooled to -50°C .

The crystallinity of the PEO/PPC polymer electrolyte membranes was calculated based on the following eq. (1)¹⁵:

$$\chi_c = \frac{\Delta H_m}{\Delta H_m^0} \times 100\% \quad (1)$$

where X_c is the percentage of crystallinity, ΔH_m^0 is the crystalline melting heat of pure PEO ($213.7\ \text{J}\ \text{g}^{-1}$), and ΔH_m is the fusion heat of PEO/PPC polymer electrolyte.

The thermal stability of the PEO/PPC polymer electrolyte ranging from 70 to 600°C was determined with a Perkin-Elmer TGA/DTA 6300 [thermogravimetric

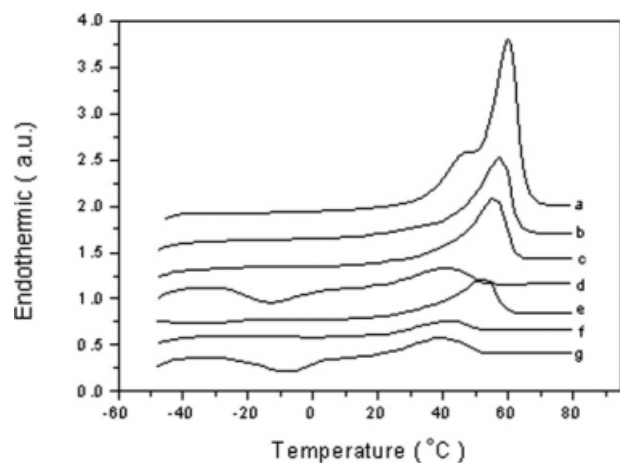


Figure 2 DSC traces for PEO/*x*%PPC polymer electrolyte: (a) *x* = 0; (b) *x* = 20; (c) *x* = 30; (d) *x* = 40; (e) *x* = 50; (f) *x* = 60; (g) *x* = 70.

analyzer (TGA)/differential thermal analysis (DTA)] under nitrogen atmosphere. The heating rate was 10°C min⁻¹.

X-ray diffraction study of the PEO/PPC polymer electrolyte was conducted with a D/Max-III X-ray diffractometer using nickel-filtered Cu K α radiation at a scan rate of 10° min⁻¹.

Ionic conductivity of the PEO/PPC electrolyte was determined by electrochemical impedance spectroscopy (EIS). The impedance tests were performed by Solartron 1255B frequency response analyzer functioning with an oscillating voltage of 5 mV from 1 MHz to 1 Hz frequency range at various temperatures ranging from 298 to 353 K. The samples were sandwiched between two polished gold disks with a diameter of 1.0 cm, which acted as ion-blocking electrodes in a specially designed cell setup for conductivity studies. The cell was placed into a self-designed oven coupled with a temperature controller. The temperature was maintained for at least 30 min before the impedance response was recorded.

The electrochemical stability of the PEO/PPC polymer electrolyte was determined using linear sweep voltammetry (LSV). The measurement was carried out with the use of a three-electrode electrochemical cell, which consisted of stainless steel (SS) working electrode, a lithium reference electrode, and

a counter electrode, and the PEO/PPC polymer electrolyte was kept between these electrodes. An electrochemical analyzer (Solartron 1255B) was operated at a scanning rate of 0.5 mV s⁻¹ and over the potential range of 3.0–6.0 V versus Li⁺/Li at room temperature. The cell was assembled in a Mikrouna Super(1220/750/900) glove box under argon atmosphere.

RESULTS AND DISCUSSION

The films formed by casting PEO, PPC, LiClO₄, and anhydrous acetone solution were auto-supported, flexible, and apparently homogeneous. It can be seen from Figure 1 that PPC domains existed as spherical shapes in the PEO matrix. This is because PEO is a crystalline polymer, but PPC is amorphous and hydrophobic. The big difference between the constituents inherent character led to the phase separation of PEO and PPC. The size of the dispersed PPC domains was in the range of 4–10 μ m for the PEO/50%PPC blend. The particle size of the dispersed PPC domains decreased with further increasing of PPC, indicating an improvement in miscibility between PPC and PEO. However, the boundary between the PPC and the PEO domains was not clear, implying good adhesion between the PPC and the PEO matrix. The improved miscibility resulted from the possible interaction between PPC and PEO.

Figure 2 and Table I present the glass transition temperature (T_g), melting point (T_m), and melting enthalpy (ΔH_m) of PEO/*x*%PPC polymer electrolytes determined by DSC measurements. The T_g of PEO decreased because of the addition of amorphous PPC. The polymer with low T_g is generally favorable to be polymer electrolyte. The physical properties such as viscosity, diffusion, and conduction become less sensitive to temperature, i.e., at temperature lower than T_g . The segmental motion of the polymeric chain increases at temperature higher than T_g , and consequently, resulting in higher ionic conductivity.

The crystalline PEO has a T_m of 60.1°C. For PEO/PPC polymer electrolytes, the T_m decreased from 60.1 to 39.4°C with increasing PPC content. The

TABLE I
Thermal Properties of PEO/PPC Polymer Electrolyte

PEO/PPC (wt %)	T_g (°C)	T_m (°C)	ΔH_m (J g ⁻¹)	X_c (%)	$T_{5\%}$ (°C)	T_{max} (°C)
100/0	-18.49	60.1	125.8	58.0	358.18	412.82
80/20	-28.4	57.6	53.81	31.5	121.68	394.26
70/30	-31.5	55.9	40.81	27.3	139.62	343.49
60/40	-	40.5	16.08	12.5	127.53	377.23
50/50	-25.7	53.8	25.8	24.0	109.64	341.50
40/60	-26.4	41.6	9.552	11.2	146.04	345.27
30/70	-	39.4	14.35	22.4	130.94	341.54

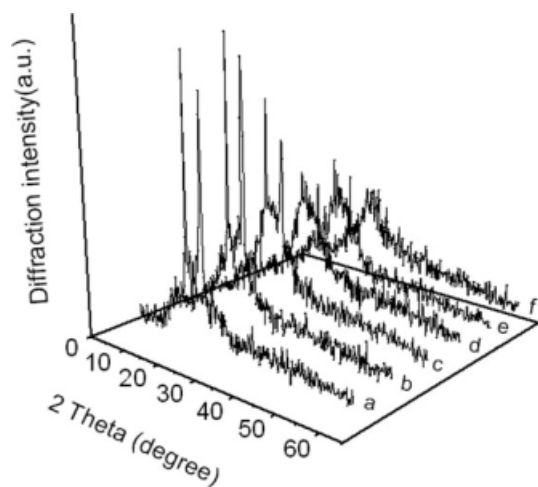


Figure 3 XRD traces of PEO/*x*%PPC polymer electrolytes: (a) *x* = 20; (b) *x* = 30; (c) *x* = 40; (d) *x* = 50; (e) *x* = 60; (f) *x* = 70.

same phenomenon was also observed for the melting enthalpy (ΔH_m), which relates with the polymer crystallinity.

The 5% weight loss temperature ($T_{5\%}$) and the maximum loss temperature (T_{max}) of the PEO/PPC polymer electrolytes obtained from the TGA measurements are tabulated in Table I. It can be seen that both $T_{5\%}$ and T_{max} of PEO/PPC polymer electrolytes tended to decrease with increasing PPC content. Two steps in the mass loss of samples correspond to the thermal decomposition of the PPC and PEO phases, respectively.

The XRD patterns for PEO/PPC polymer electrolyte are shown in Figure 3. Two sharp peaks are observed at $2\theta = 19^\circ$ and 25° , corresponding to the crystalline-phase PEO. It is apparent that crystallinity of PEO/PPC polymer electrolyte decreased dramatically with increasing PPC content. The resulted amorphous nature is beneficial to the diffusion of ions in the polymer electrolyte and results in the high conductivity.

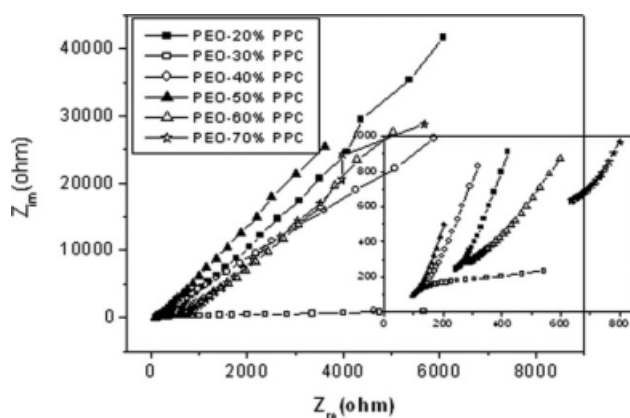


Figure 4 Nyquist plots for PEO/*x*%PPC/10%LiClO₄ polymer electrolyte at room temperature.

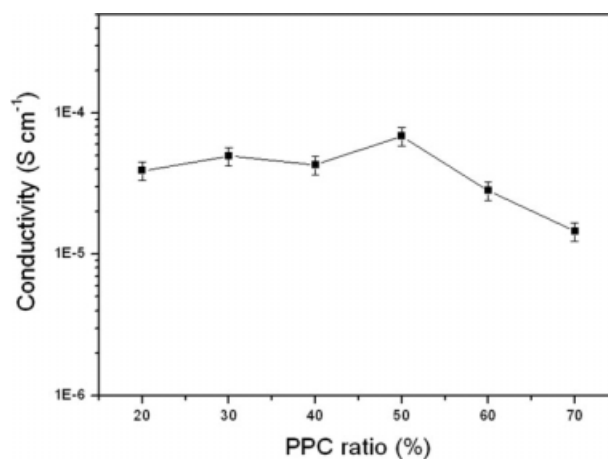


Figure 5 Ionic conductivity of PEO/*x*%PPC/10%LiClO₄ polymer electrolyte.

The ionic conductivity was determined by electrochemical impedance spectroscopy (EIS) analysis. Figure 4 shows the Nyquist plots of PEO/*x*%PPC polymer electrolyte at room temperature. The impedance spectra of all PEO/PPC polymer electrolytes are almost linear starting from the real axis. The disappearance of semicircular portion in the high frequency range, as shown in the inset of Figure 4, suggests that the current carriers are ions according to theoretical analysis.²³ This behavior was often observed in the impedance response of PEO-type polymer electrolytes.^{24,25}

Hence, the resistance R_b can be estimated from the impedance spectra at the point where the line intercepted the real part in the high-frequency region. The ionic conductivity was calculated using the following equation:

$$\sigma = \frac{d(\text{cm})}{R_b(\Omega)S(\text{cm}^2)}$$

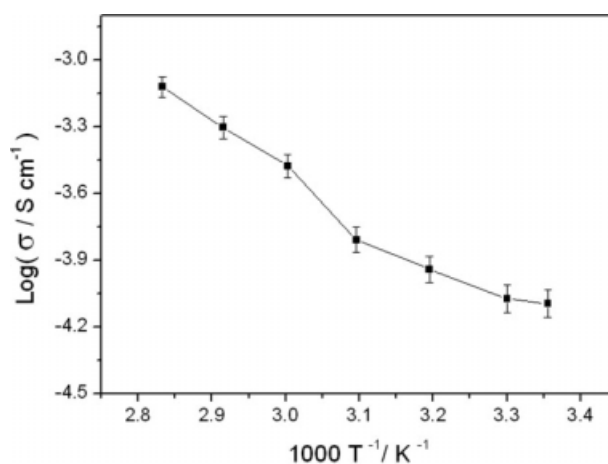


Figure 6 Temperature dependence of ionic conductivity for PEO/50%PPC/10%LiClO₄ polymer electrolyte.

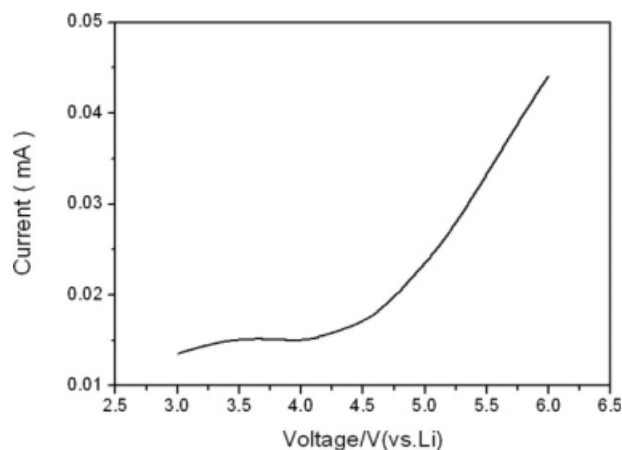


Figure 7 Linear sweep voltammogram curve of PEO/50%PPC/10%LiClO₄ polymer electrolyte.

where σ is the ionic conductivity, d is the thickness of the polymer electrolyte, R_b is the resistance of bulk electrolyte estimated from the Nyquist plot, and S is the area of the polished gold electrode.

Figure 5 shows the variations of the ionic conductivity of the PEO/PPC/10%LiClO₄ polymer electrolytes versus PPC content at room temperature. The results indicate that the incorporation of PPC gives a great rise in ionic conductivity. The ionic conductivity of the PEO/PPC polymer electrolyte increases with increasing PPC content, up to a maximum value at 50 wt % PPC used. The highest ionic conductivity of PEO/50%PPC polymer electrolyte is $6.83 \times 10^{-5} \text{ S cm}^{-1}$ at room temperature. Then, the ionic conductivity decreased with further increase of PPC content. This result is consistently well with the change of ΔH_m and crystallinity of PEO/PPC polymer electrolyte observed in Table I and Figures 2 and 3. The crystallinity of PEO/PPC polymer electrolyte is considered to be the major factor to improve the ionic conductivity.

The temperature dependence of the ionic conductivity of the PEO/PPC polymer electrolyte was performed at temperature range of 298–353 K. Typical plot of ionic conductivity versus inverse temperature ($1000/T$) for PEO/50%PPC polymer electrolyte at different temperature is shown in Figure 6. In general, the ionic conductivity increases with the increase of temperature, and it obeys the Arrhenius plot of conductivity. The ionic conductivities of other PEO/PPC polymer electrolytes exhibited similar behavior. The completely amorphous nature of this polymer electrolyte can promote the motion of lithium ion in the polymer network.

The electrochemical stability window of PEO/50%PPC/10%LiClO₄ polymer electrolyte was studied by LSV as shown in Figure 7. It can be seen from the voltammogram curve that the decomposition voltage of PEO/50%PPC/10%LiClO₄ polymer electrolyte is around 4.5 V versus Li/Li⁺.

CONCLUSIONS

The PEO/PPC polymer electrolytes can be readily fabricated by solution-casting technique. Experimental results indicated that the ionic conductivity of the PEO/PPC polymer electrolyte increased with increasing PPC content, up to a maximum value of $6.83 \times 10^{-5} \text{ S cm}^{-1}$ at room temperature for PEO/50%PPC polymer electrolyte. Then, the ionic conductivity decreased with further increase of PPC content. The dependence of the ionic conductivity on temperature obeys the Arrhenius plot of conductivity. The crystallinity of PEO phase in PEO/PPC blends decreased with increasing PPC content, resulting in the increase in the ionic conductivity. The LSV study demonstrated that the PEO/50%PPC polymer electrolyte exhibited good electrochemical stability up to 4.5 V.

References

- Scrosati, B. *Electrochim Acta* 2000, 45, 2461.
- Sato, T.; Bannob, K.; Maruob, T.; Nozub, R. *J Power Sources* 2005, 152, 264.
- Sivakkumar, S. R.; Saraswathi, R. *J Power Sources* 2004, 137, 322.
- Stephan, A. M.; Nahm, K. S. *Polymer* 2006, 47, 5952.
- Kenji, N.; Yoshimasa, K.; Youshin, Y.; Kensuke, H. *Eur. Pat. Appl. EP 1,211,747* (2002).
- Xu, J. J.; Ye, H.; Huang, J. *Electrochem Commun* 2005, 7, 1309.
- Itoh, T.; Mitsuda, Y.; Nakasaka, K.; Uno, T.; Kubo, M.; Yamamoto, O. *J Power Sources* 2006, 163, 252.
- Jayathilaka, P. A. R. D.; Dissanayake, M. A. K. L.; Albinsson, I.; Mellander, B.-E. *Solid State Ionics* 2003, 156, 179.
- Rajendran, S.; Sivakumar, P. *Phys B: Condens Matter* 2008, 403, 509.
- Subramania, A.; Kalyana, N. T.; Sathiya Priya, A. R.; Vijaya Kumar, G. *J Membr Sci* 2007, 294, 8.
- Zhang, H. P.; Zhang, P.; Li, Z. H.; Sun, M.; Wu, Y. P.; Wu, H. Q. *Electrochem Commun* 2007, 9, 1700.
- Fonseca, C. P.; Rosa, D. S.; Gaboardi, F.; Neves, S. *J Power Sources* 2006, 155, 381.
- Sivakumar, M.; Subadevi, R.; Rajendran, S.; Wu, H. C.; Wu, N. L. *Eur Polym J* 2007, 43, 4466.
- Wen, T. C.; Chen, W. C. *J Power Sources* 2001, 92, 139.
- Ciosek, M.; Siekierski, M.; Wiczeorek, W. *Electrochim Acta* 2005, 50, 3922.
- Scrosati, B.; Croce, F.; Persi, L. *J Electrochem Soc* 2000, 147, 1718.
- Dias, F. B.; Plomp, L.; Veldhuis, J. B. J. *J Power Sources* 2000, 88, 169.
- Xi, J. Y.; Qiu, X. P.; Cui, M. Z.; Tang, X. Z.; Zhu, W. T.; Chen, L. Q. *J Power Sources* 2006, 156, 581.
- Polo Fonseca, C.; Cezare, T. T.; Neves, S. *J Power Sources* 2002, 112, 395.
- Christie, A. M.; Lilley, S. J.; Staunton, E.; Adreev, Y. G.; Bruce, P. G. *Nature* 2005, 433, 50.
- Wang, X. L.; Mei, A.; Li, X. L.; Lin, Y. H.; Nan, C. W. *J Power Sources* 2007, 171, 913.
- Du, L. C.; Meng, Y. Z.; Wang, S. J.; Tjong, S. C. *J Appl Polym Sci* 2004, 90, 1840.
- Macdonald, J. R. *J Chem Phys* 1974, 61, 3977.
- Appetecchi, G. B.; Zane, D.; Scrosati, B. *J Electrochem Soc* 2004, 151, A1369.
- Wang, M. K.; Dong, S. J. *J Power Sources* 2007, 170, 425.